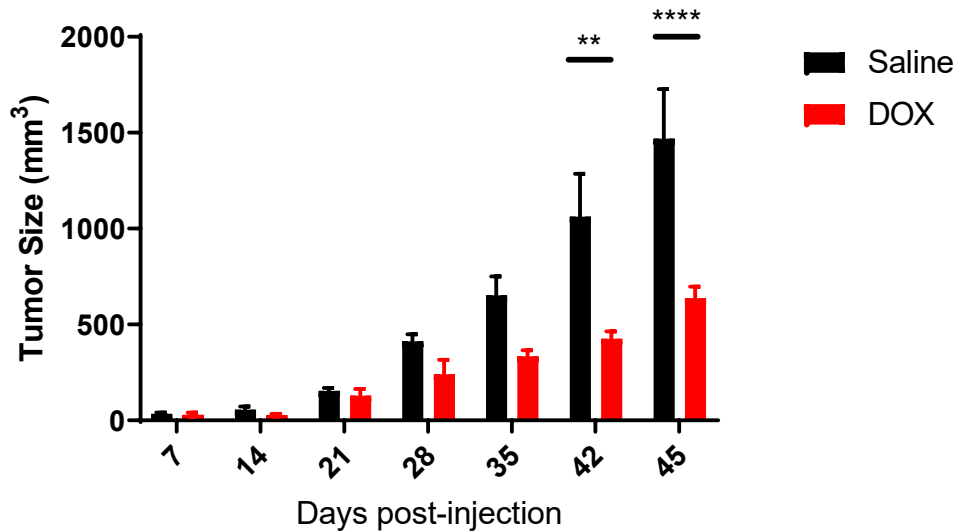


Supplementary data

HDAC6 inhibition reverses long-term doxorubicin-induced cognitive dysfunction by restoring microglia homeostasis and synaptic integrity

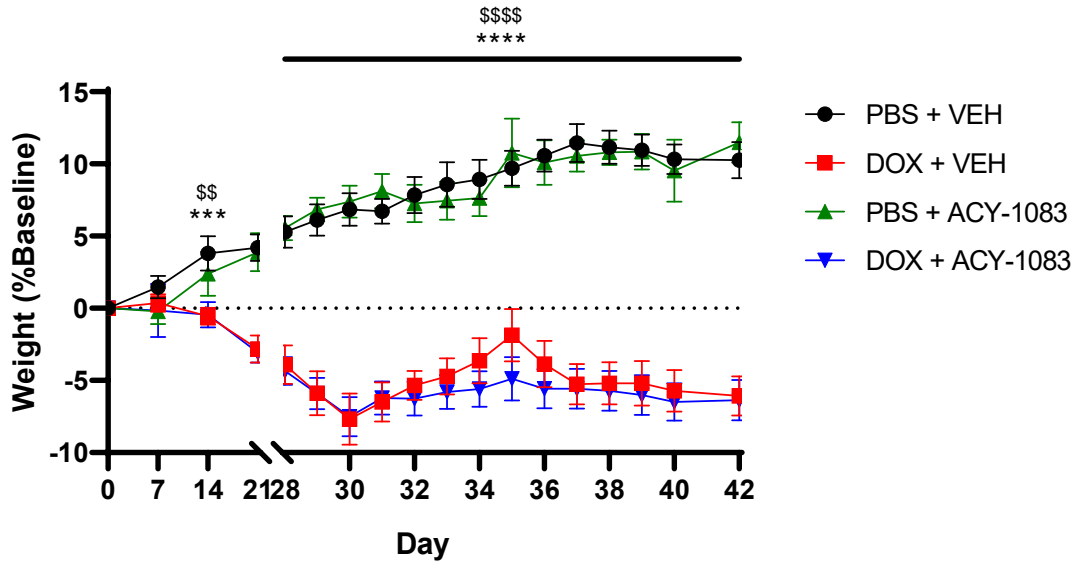
Blake R McAlpin, Rajasekaran Mahalingam, Anand K Singh, Shruti Dharmaraj, Taylor T Chrisikos, Nabila Boukelmoune, Annemieke Kavelaars, and Cobi J Heijnen



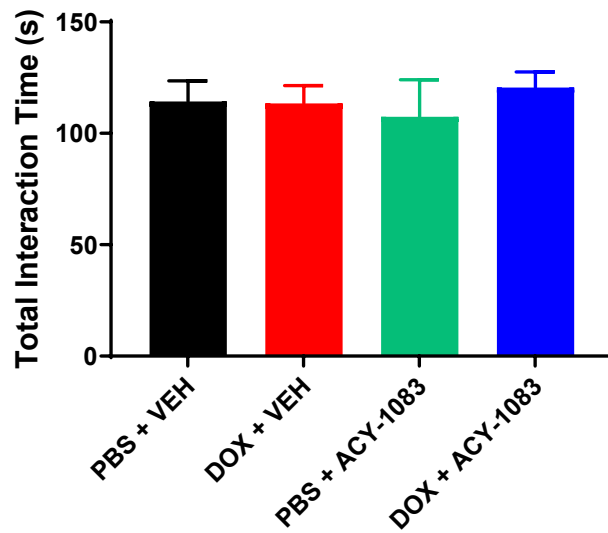
Supplementary Figure 1. Doxorubicin inhibition of tumor growth *in vivo* in a PyMT breast cancer model. On day 0, 2.5×10^5 PyMT cells were injected in the 4th mammary fat pad.

Doxorubicin treatment began at day 28. Results are expressed as mean \pm SEM; n = 4

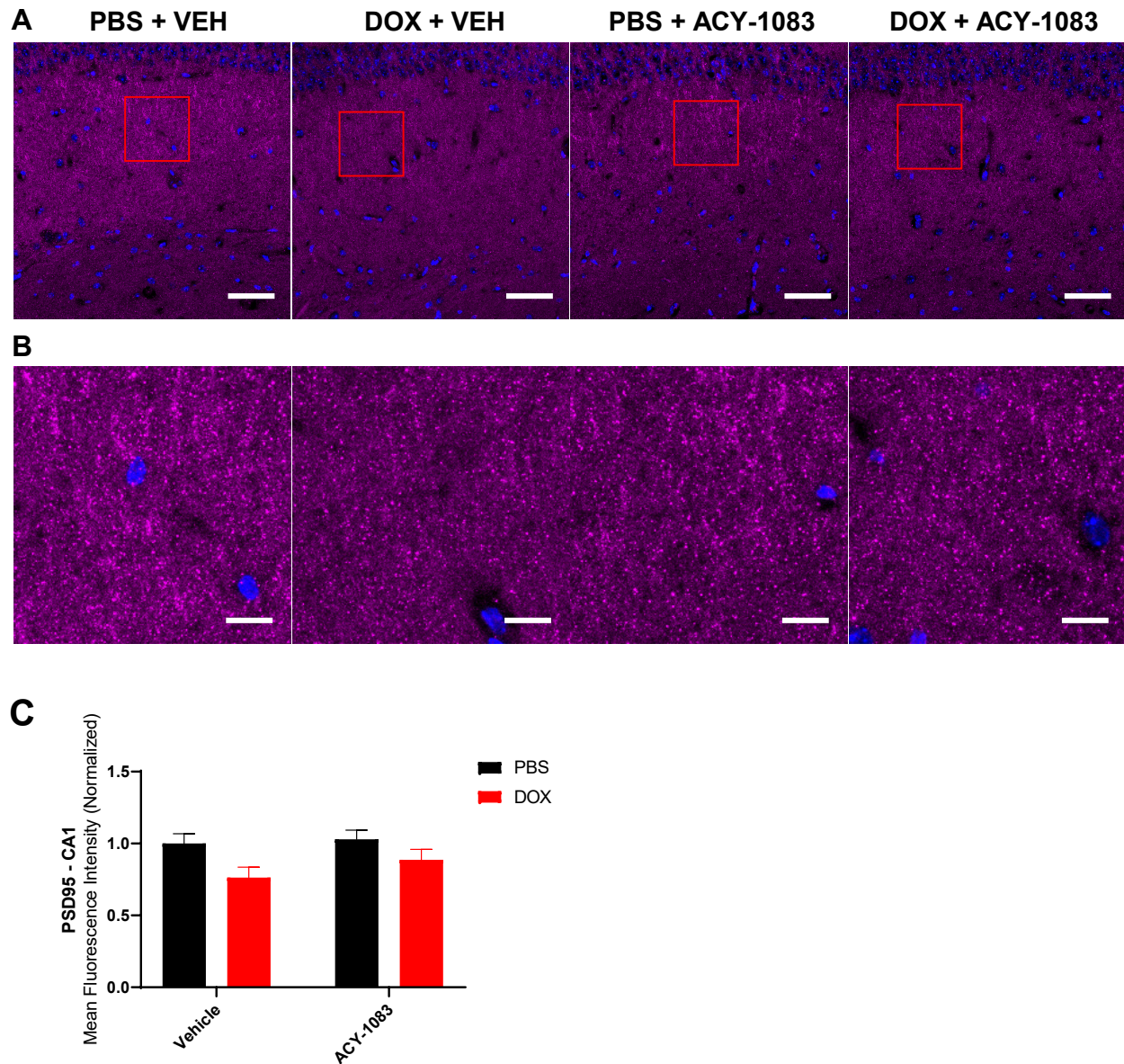
mice/group; Unpaired t test **p \leq 0.01; **** p \leq 0.0001.



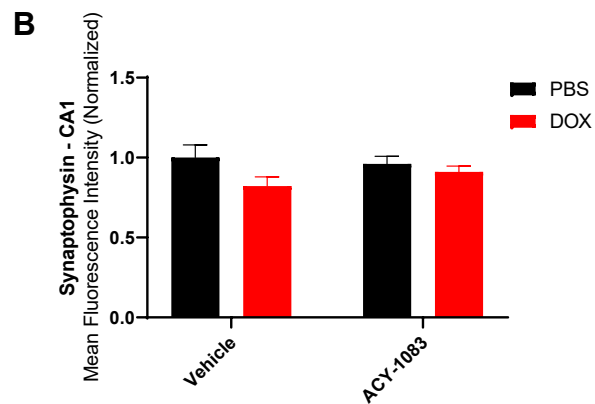
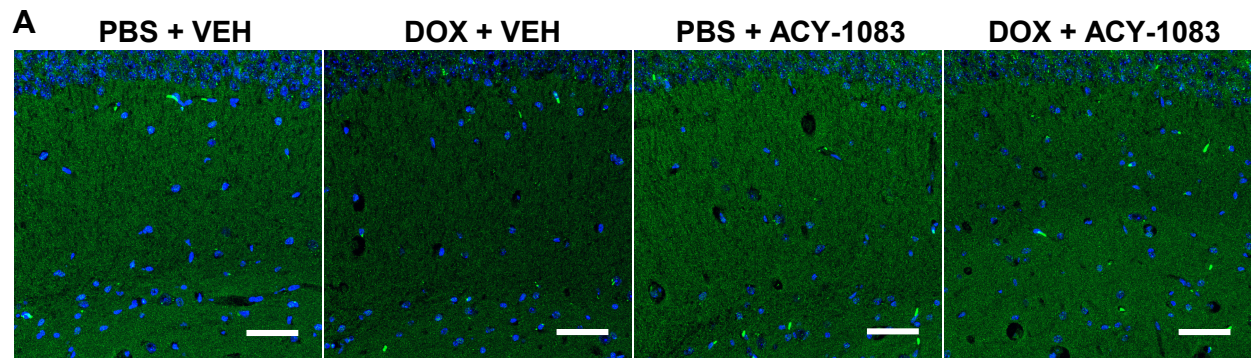
Supplementary Figure 2. Percentage of baseline body weight was recorded. Results are expressed as means \pm SEM; n = 5-11 mice/group; Two-way ANOVA with Tukey's post hoc analysis; *** $p \leq 0.001$; **** $p \leq 0.0001$ PBS/VEH vs. DOX/VEH and PBS/VEH vs DOX/ACY-1083; \$\$\$ $p \leq 0.01$; \$\$\$\$ $p \leq 0.0001$ PBS/ACY-1083 vs. DOX/VEH and PBS/ACY-1083 vs. DOX/ACY-1083.



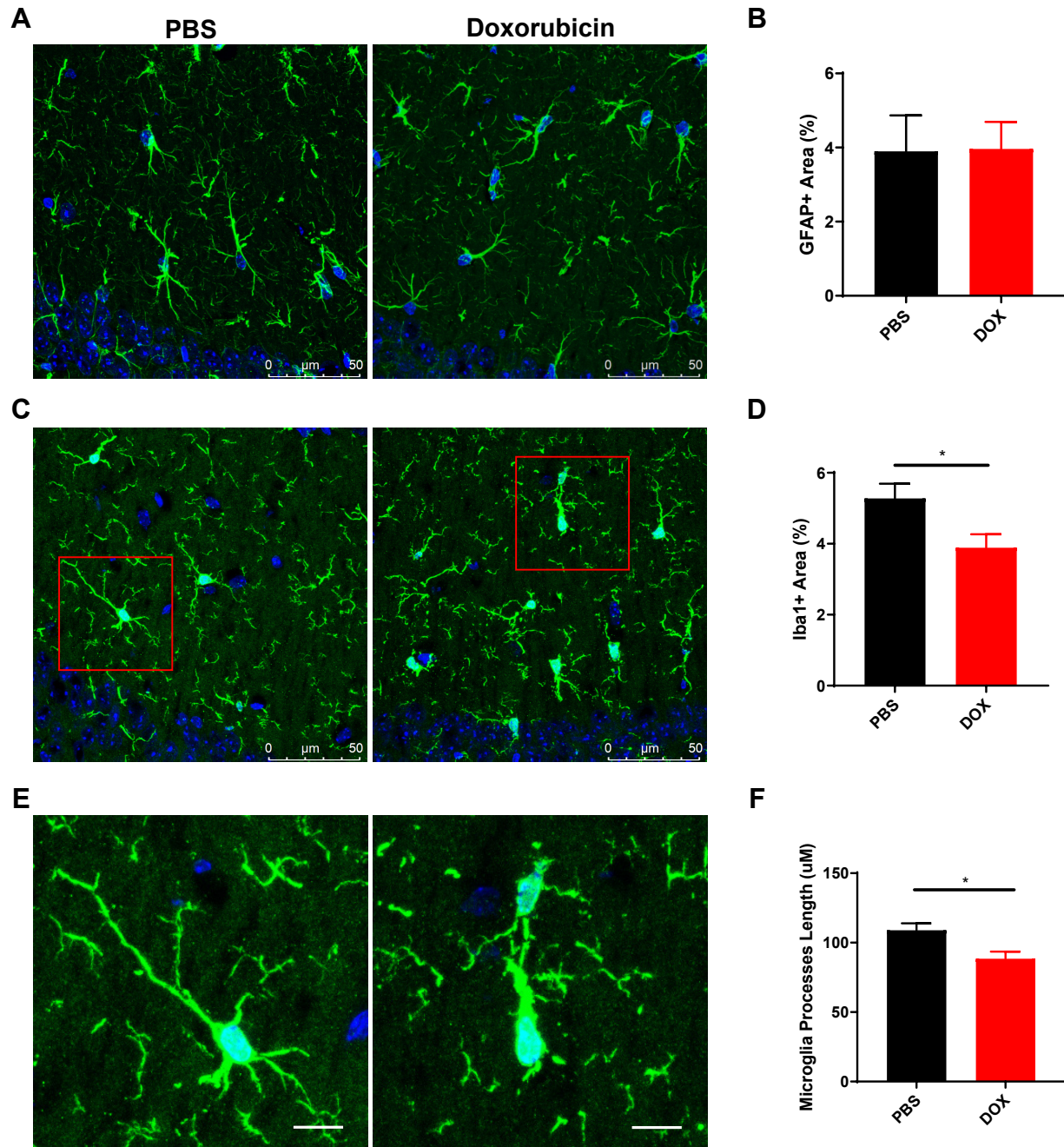
Supplementary Figure 3. Total interaction time with both novel and familiar objects in the novel object place recognition test. Results are expressed as mean \pm SEM; n = 8-16 mice/group; Two-way ANOVA with Tukey's post hoc analysis.



Supplementary Figure 4. PSD95 expression in the CA1 of the hippocampus. **(A)** Mouse CA1 hippocampal region stained with PSD95 for different treatment groups; scale bars 50 μm ; magnification 40x. **(B)** Higher magnification ROI reveals PSD95+ synaptic puncta; scale bars 10 μm . **(C)** Quantification of the mean fluorescence intensity of PSD95+ puncta. Results are expressed as mean \pm SEM; n = 9-14 mice/group; Two-way ANOVA with Tukey's post hoc analysis.

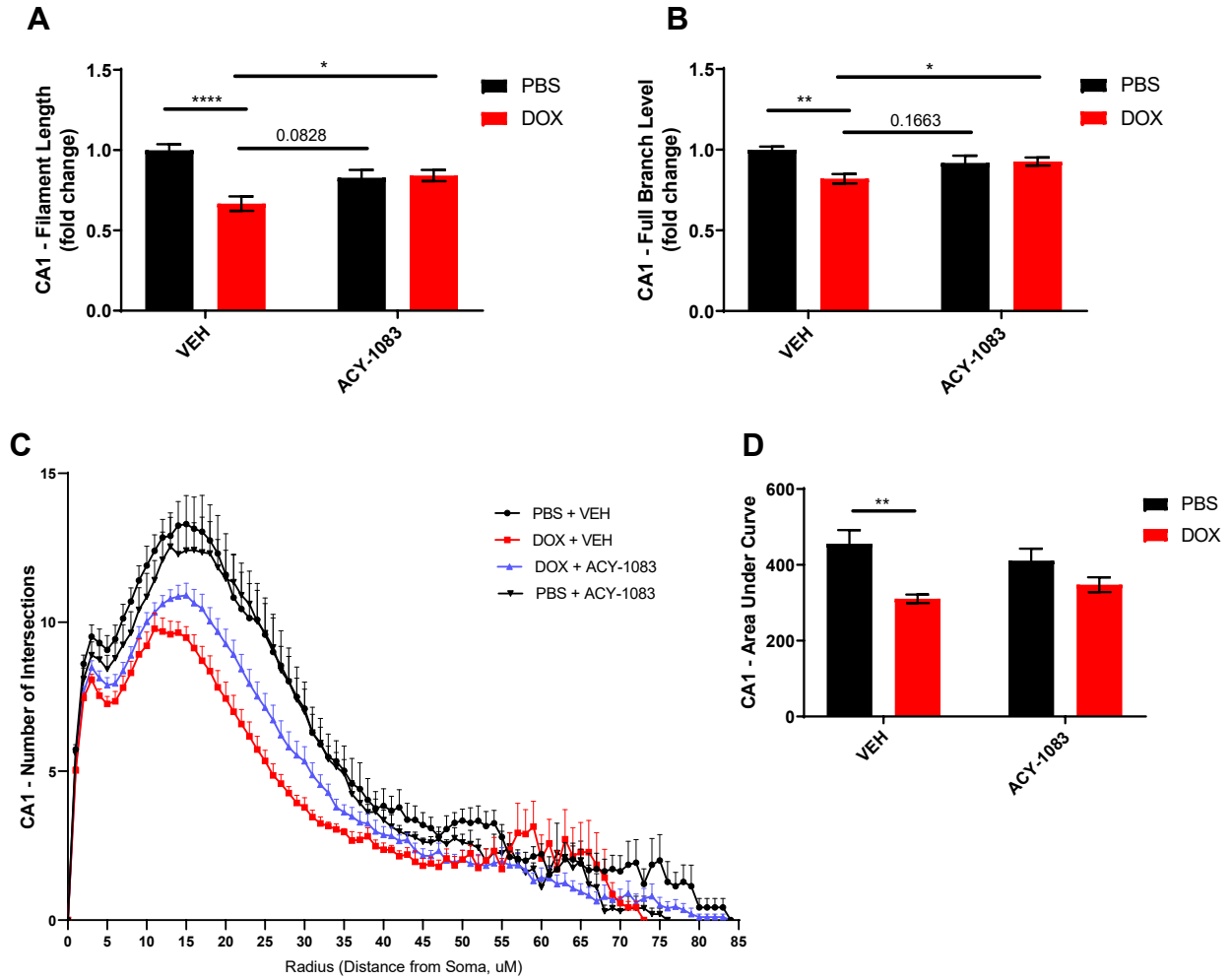


Supplementary Figure 5. Synaptophysin expression in the CA1 of the hippocampus. **(A)** Mouse CA1 hippocampal region stained with synaptophysin for different treatment groups; scale bars 50 μ m; magnification 40x. **(B)** Quantification of the mean fluorescence intensity of synaptophysin staining. Results are expressed as mean \pm SEM; n = 7-9 mice/group; Two-way ANOVA with Tukey's post hoc analysis.



Supplementary Figure 6. (A) 8 μm -thick mouse hippocampal sections stained with GFAP to visualize astrocyte morphology; scale bars 50 μm . **(B)** Percentage of GFAP+ staining area was unchanged following doxorubicin treatment. **(C)** 8 μm -thick mouse hippocampal sections stained with Iba1 to visualize microglia morphology; scale bars 50 μm ;

magnification 40x. **(D)** Percentage of Iba1+ staining area was decreased following doxorubicin treatment. **(E)** Higher magnification ROI reveals an altered microglia morphology and **(F)** significant decrease in microglia projection length; scale bars 10 μm . Results are expressed as mean \pm SEM; n = 4 mice/group; Unpaired t test *p \leq 0.05.



Supplementary Figure 7. ACY-1083 reverses doxorubicin-induced alterations in microglia

morphology in the CA1 region of the hippocampus. **(A)** Filament length of CA1 microglia.

(B) Full branch level of CA1 microglia. **(C)** Sholl analysis of CA1 microglia. **(D)**

Quantification of area under the Sholl curve from C. Results are expressed as mean \pm SEM; n

= 5-10 mice/group; Two-way ANOVA with Tukey's post hoc analysis * $p \leq 0.05$; ** $p \leq 0.01$;

**** $p \leq 0.0001$.